

From Brain to mind – experiments-> principles -> equations

Mikhail Rabinovich

Lecture # 1

October 12 2015

San Diego

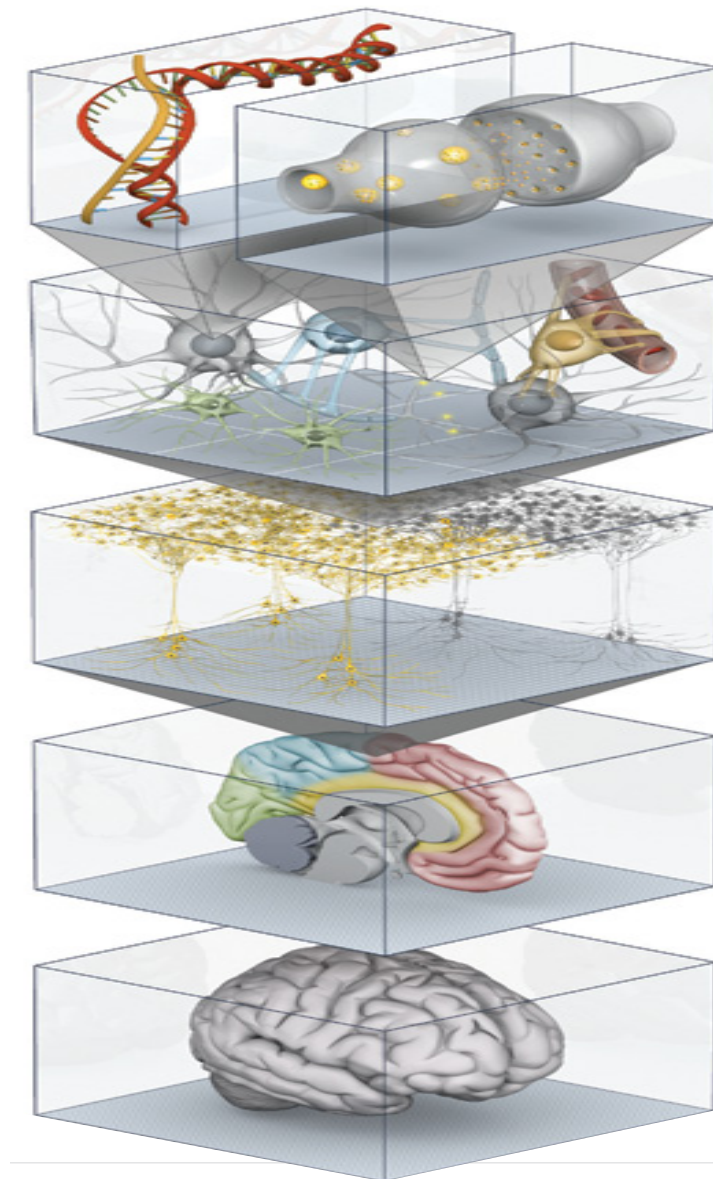


Photo credit: EPFL/HBP

Brain complexity

The average human brain has about ***100 billion neurons*** (or nerve cells) and many more neuroglia (or glial cells) which serve to support and protect the neurons (although see the end of this page for more information on glial cells). Each neuron may be connected to up to ***10,000 other neurons***, passing signals to each other via as many as ***1,000 trillion synaptic connections***, equivalent by some estimates to a computer with a 1 trillion bit per second processor. Estimates of the human brain's memory capacity vary wildly from 1 to 1,000 terabytes (for comparison, the 19 million volumes in the US Library of Congress represents about 10 terabytes of data).

Levels of modeling



molecular

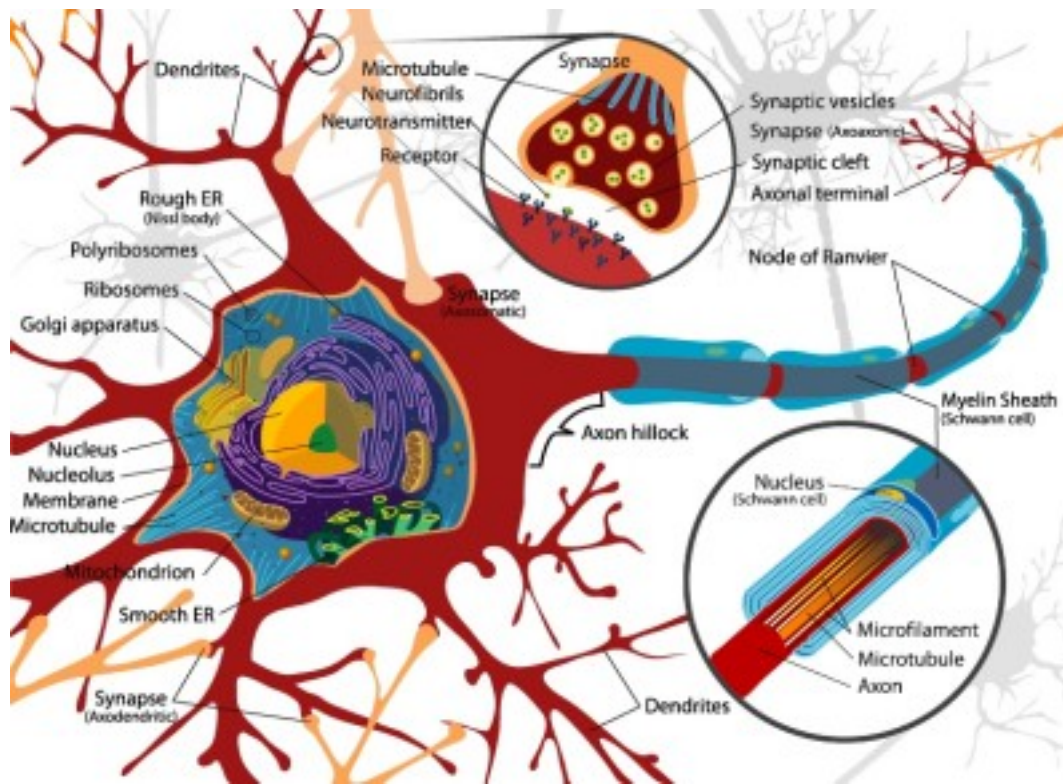
cellular

circuits

regions

whole brain

Diagram of a neuron

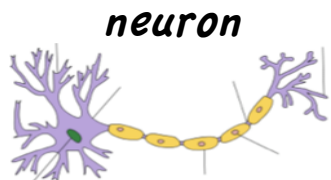


from Wikipedia (<http://en.wikipedia.org/wiki/Neuron>)

Space-Time Hierarchy in The Brain

Scale

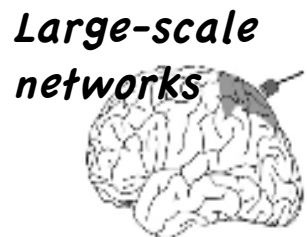
Microscopic



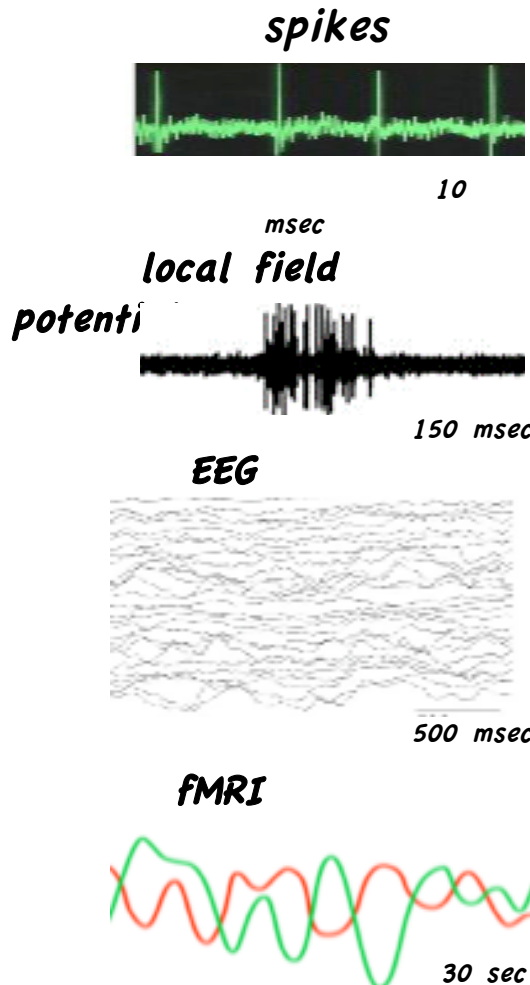
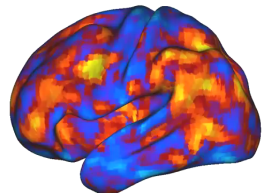
Mesoscopic
macrocolumn- 8000



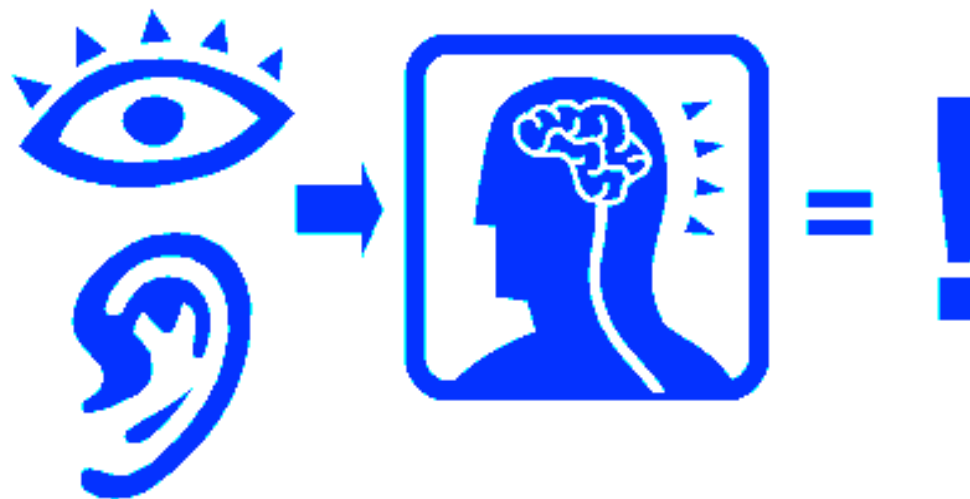
Macroscopic
cortical region, $\text{cm}^3 > 100\ 000 - 1\ \text{million}$



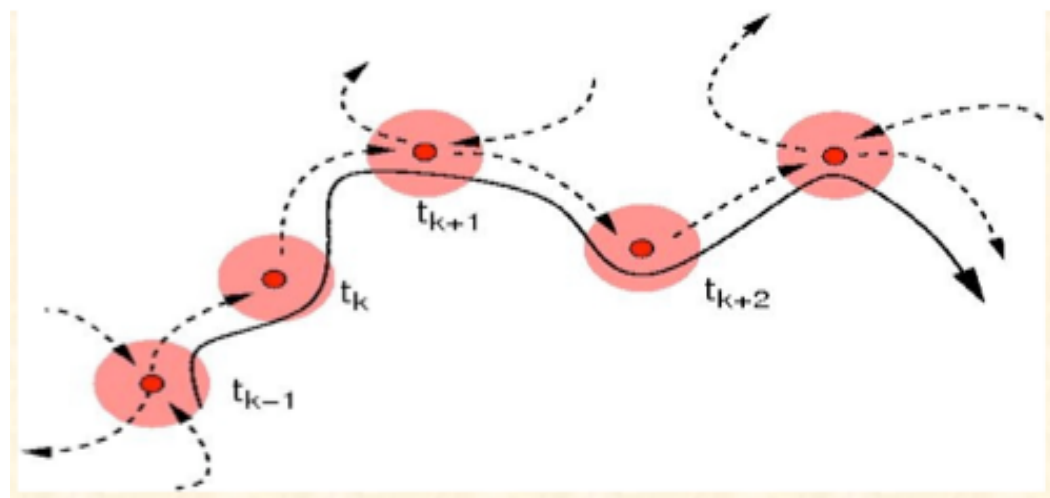
Global mode
interactions



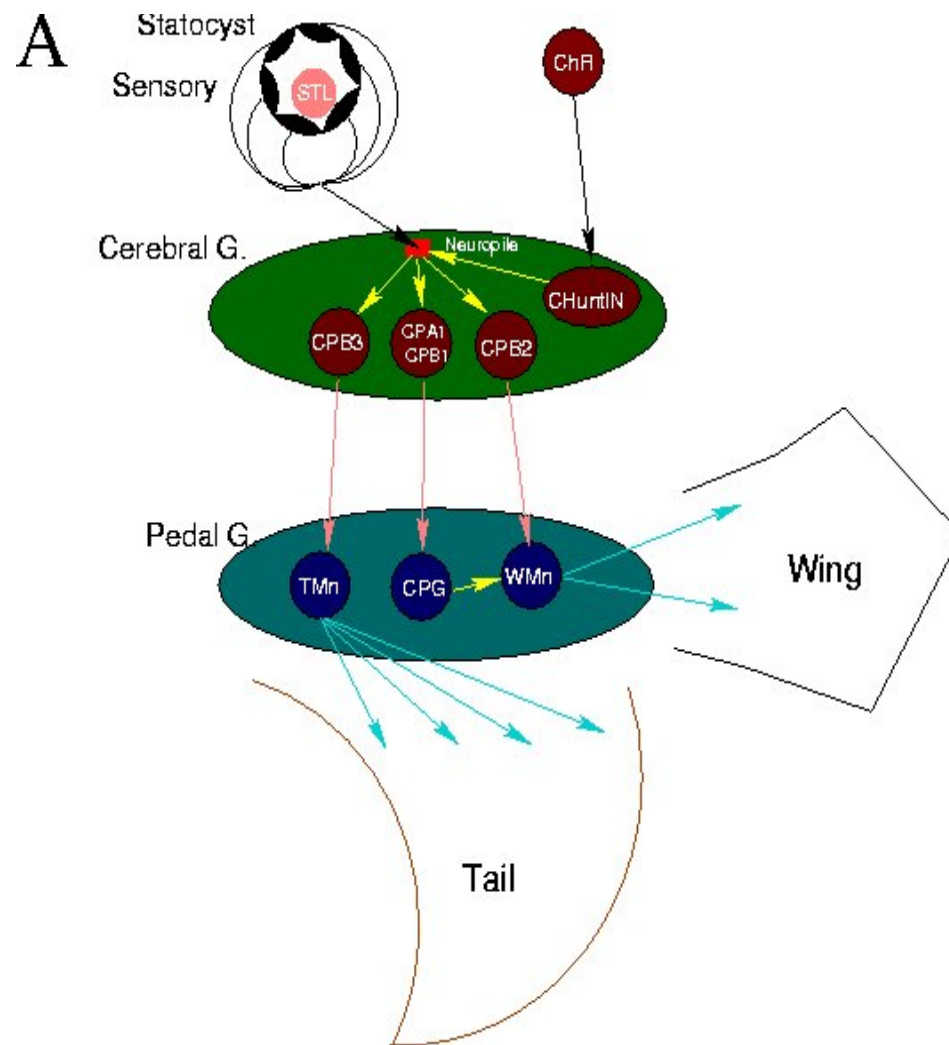
Cognitive Sequential Dynamics is the Dynamics that leads agent to the specific Goal



The flow of information in cognitive space between sequential sub-processes

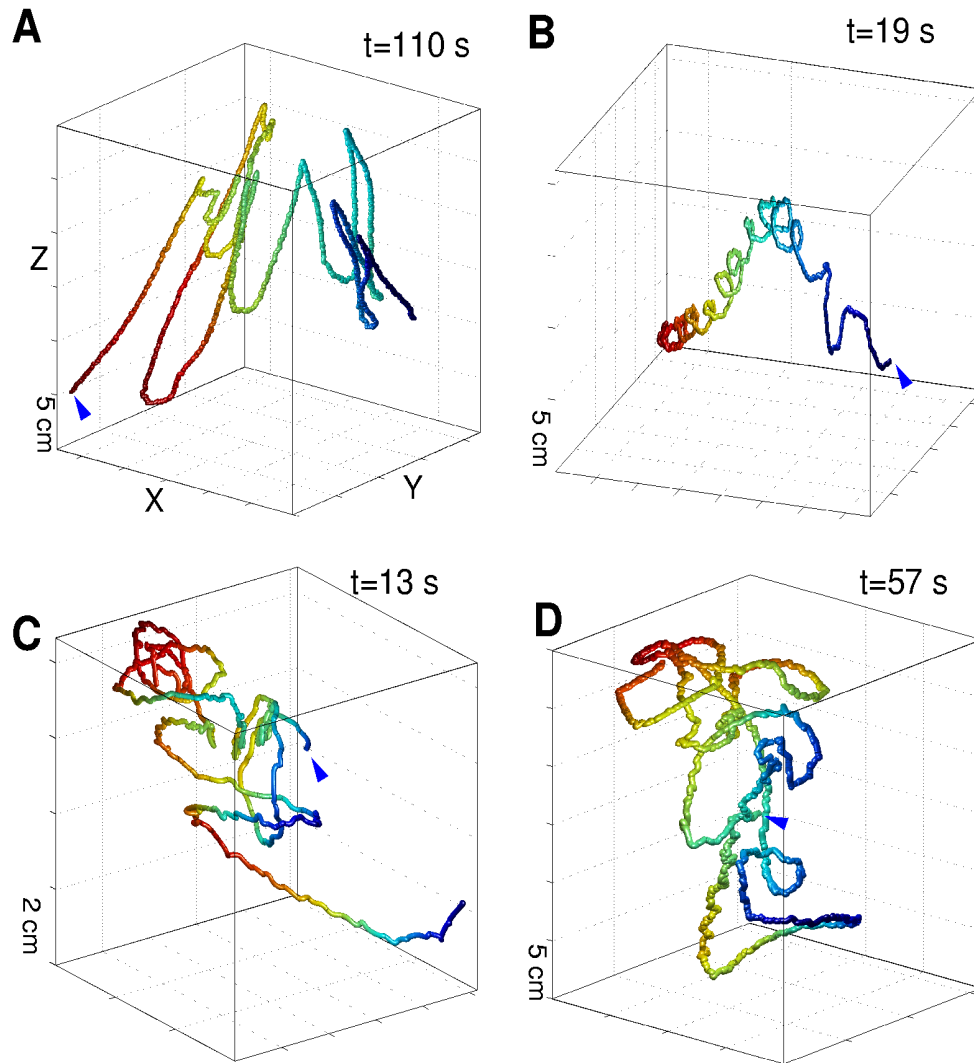


From sensory input to complex behavior

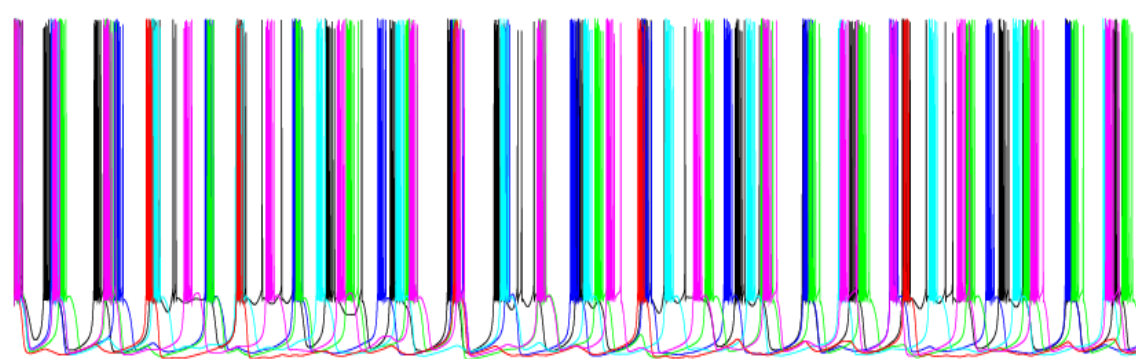
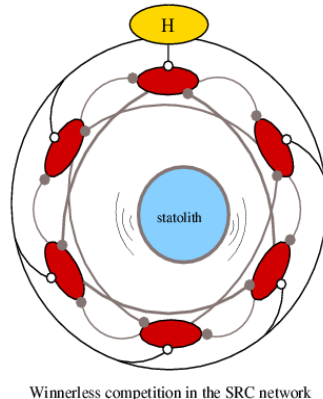
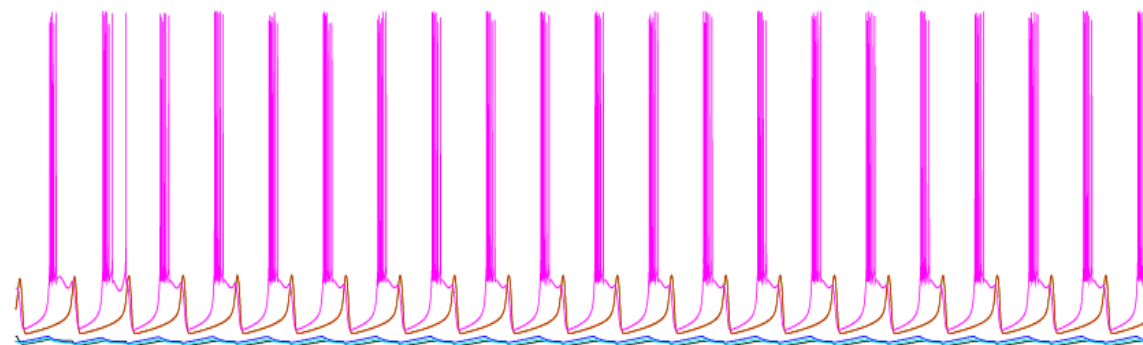
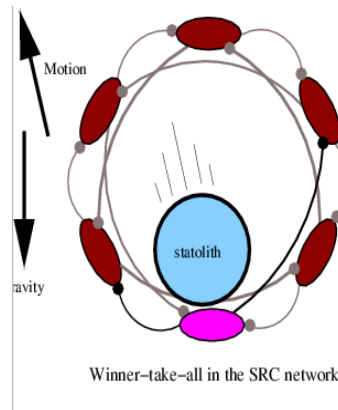


Levi, Varona, Arshavsky, Rabinovich, Selverston, Dual Sensory-Motor Function for a Molluskan Statocyst Network. *J Neurophysiol* 91: 336–345, 2004.

CLIONE's Hunting behavior

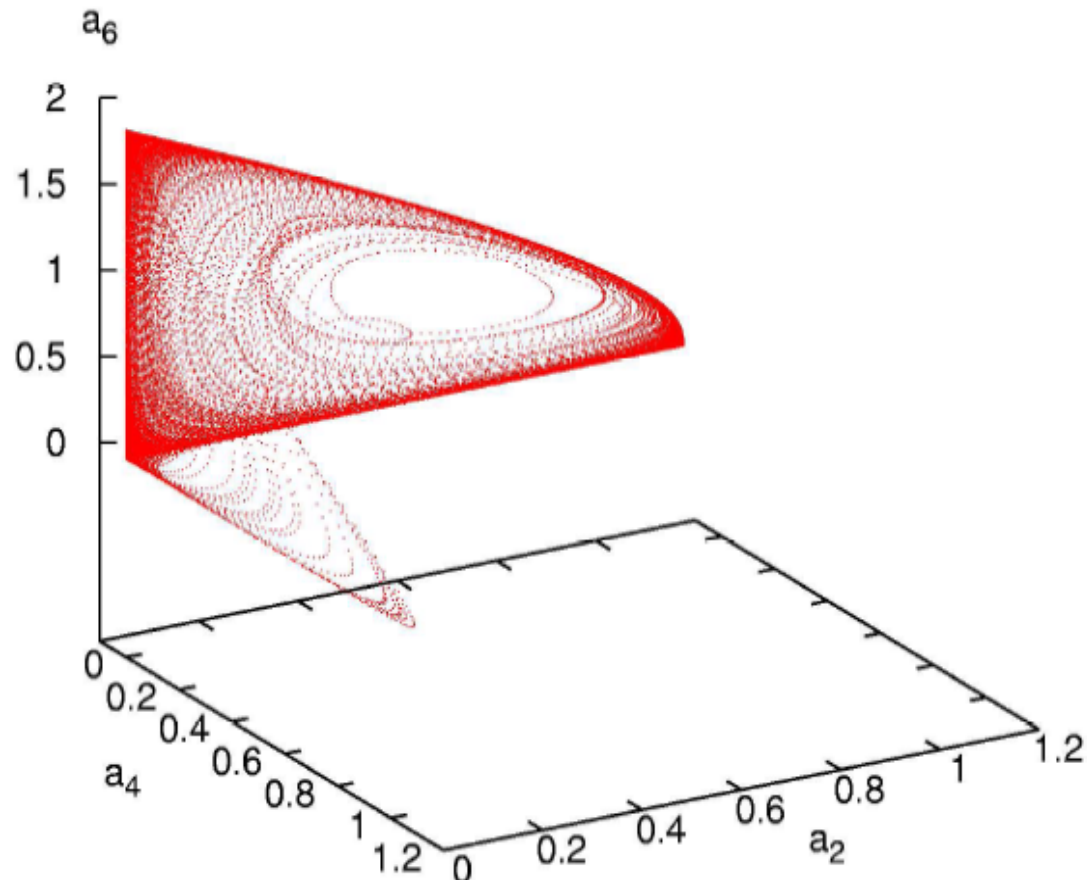


Dual function of the statocyst Clione network



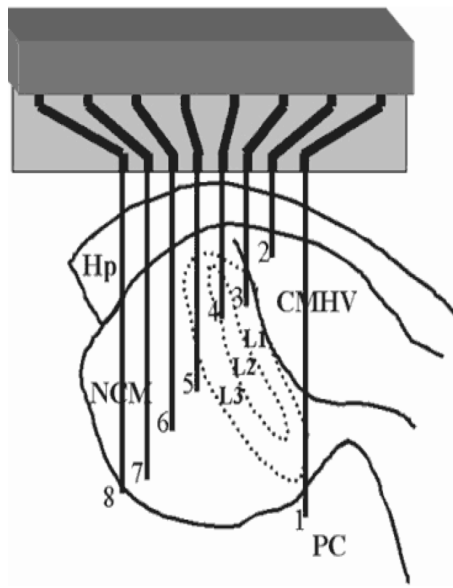
Levi, Varona, Arshavsky, Rabinovich, Selverston. The Role of Sensory Network Dynamics in Generating a Motor Program. *Journal of Neuroscience*, 2005 • 25(42):9807–9815.

Chaotic CLIONE hunting in the model



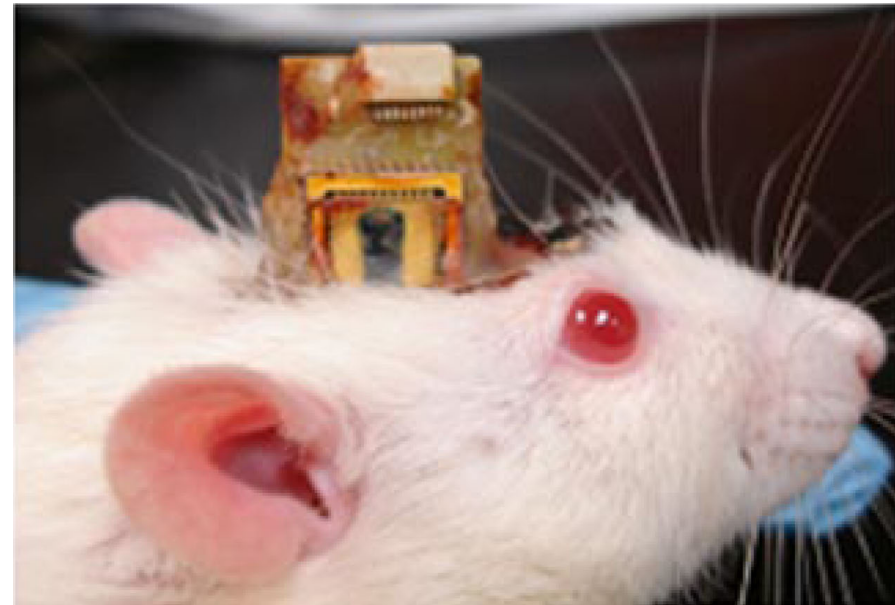
Varona P. Levi R. Arshavsky YI. Rabinovich MI. Selverston AI. Competing sensory neurons and motor rhythm coordination. Neurocomputing. 58-60:549-554, 2004

As a model of some cognitive functions in the human brain one can use an animal brain



Electrodes in different connected parts of the songbird auditory forebrain.

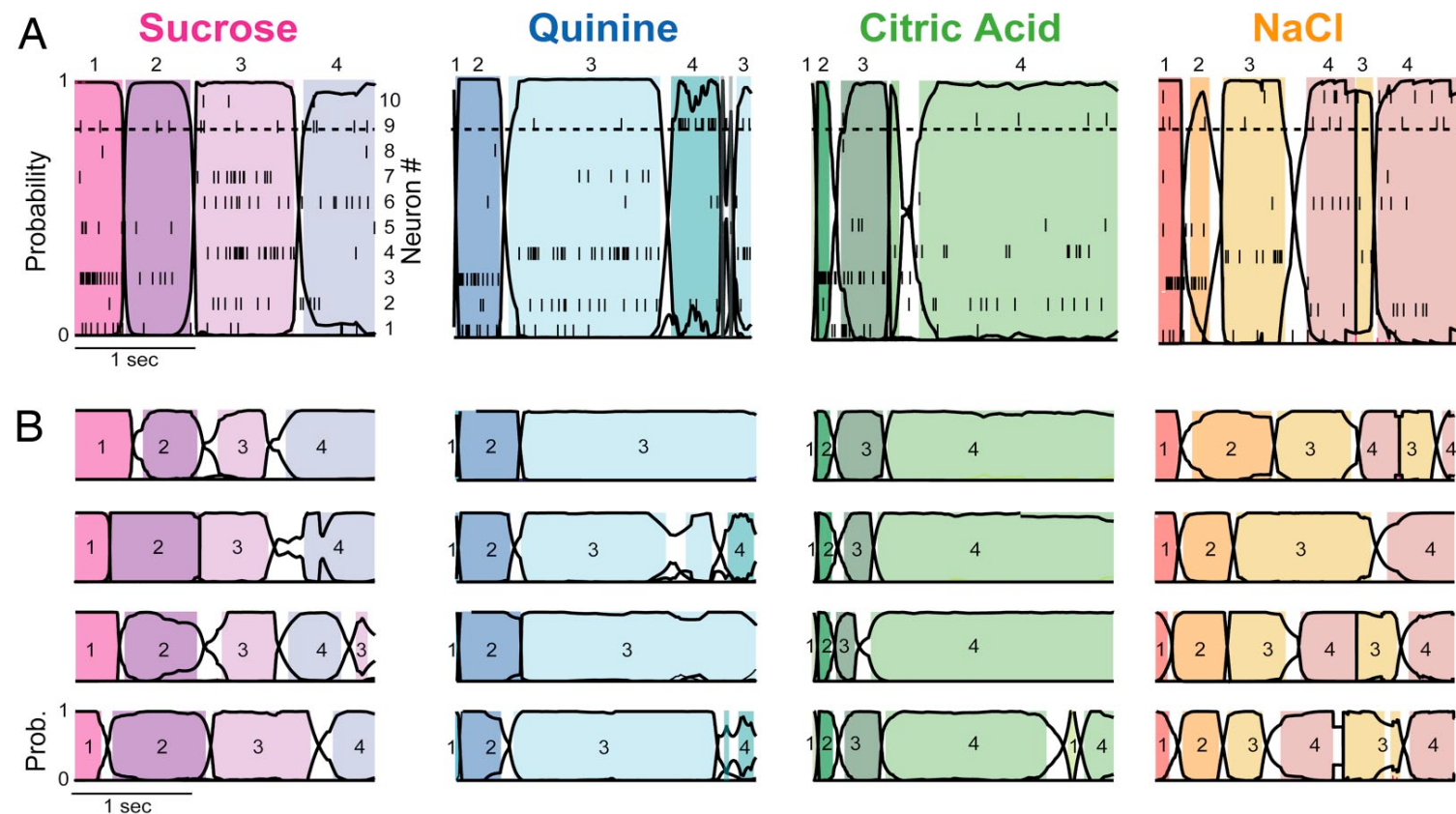
From Jarvis, *Ann. N.Y. Acad. Sci* 1026: 749-777 (2004).



Movable microelectrodes offer many advantages over stationary microelectrodes. *Nathan Jeckson et al. (2010)*

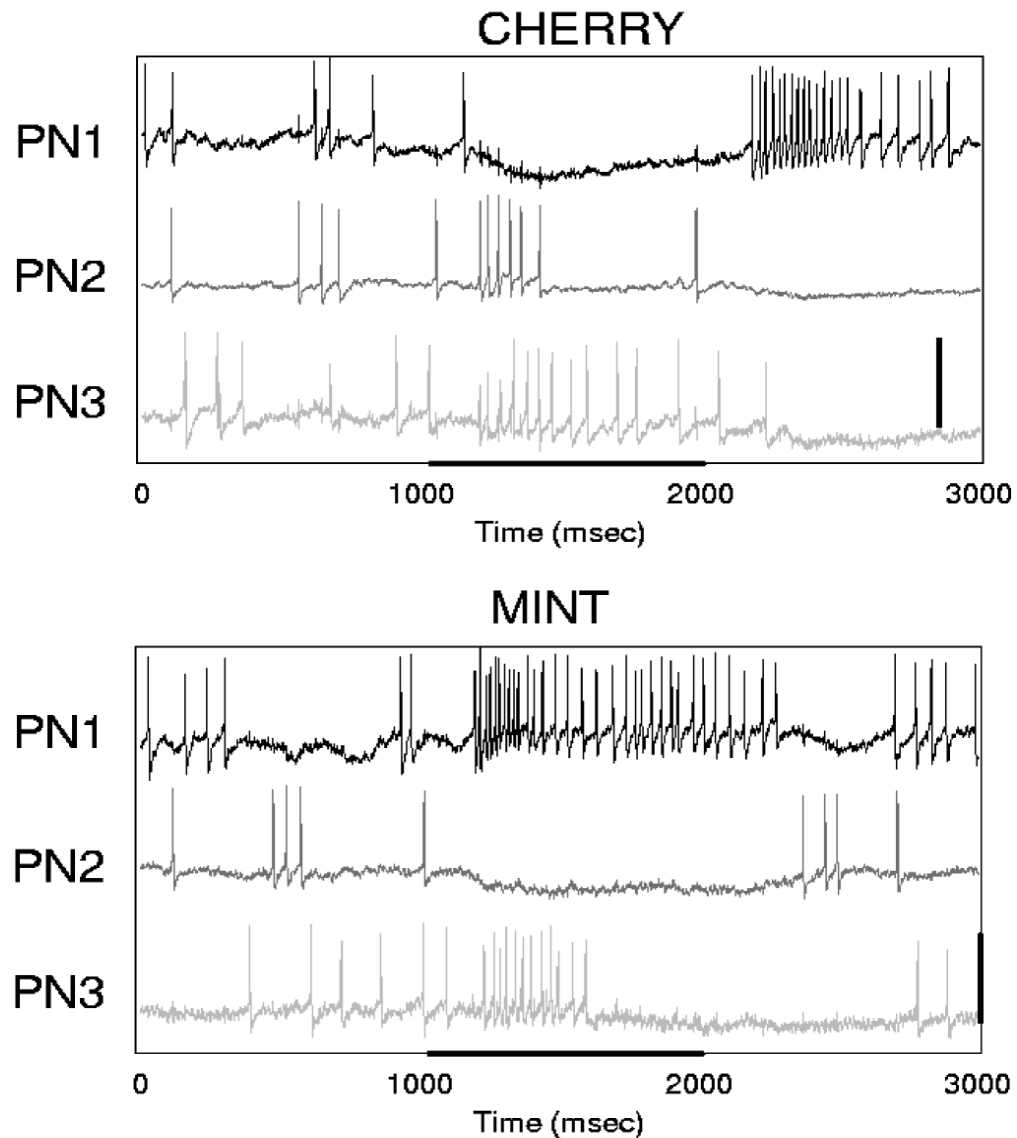
Representation of the Tastes by Transients

- (A) Stimulus-specific sequences in GC for 4 different tastes ;
(B) The sequences of metastable states are reproducible in spite of the irregularity in their switching times (Jones et al PNAS 2007).

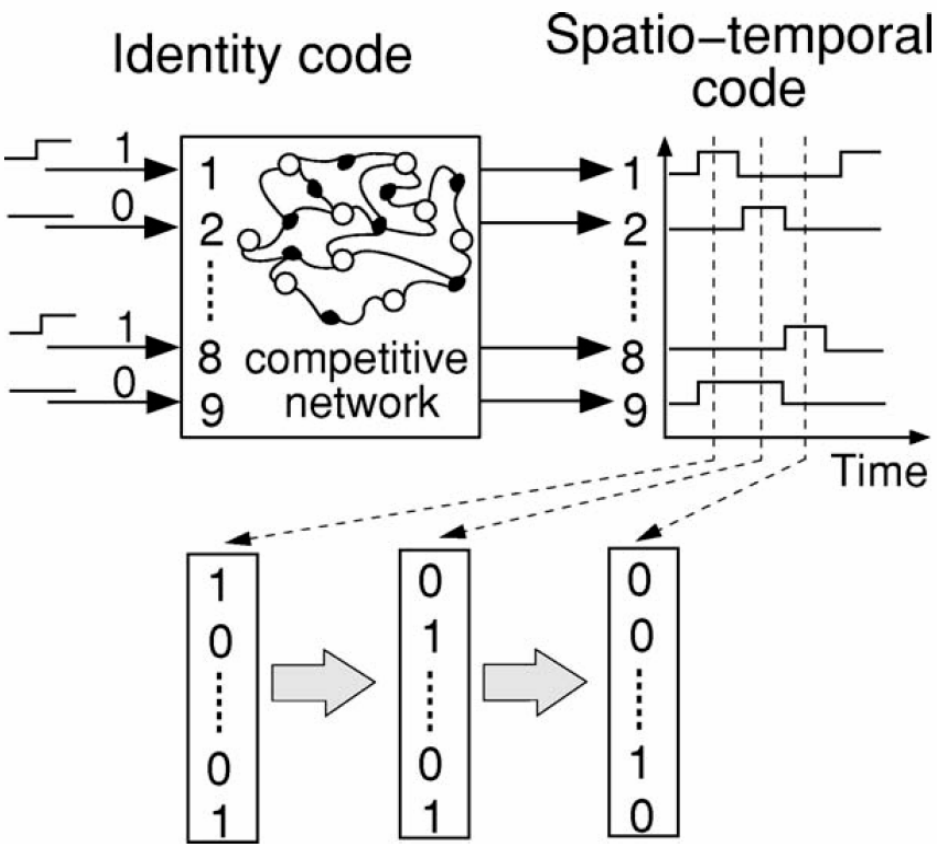


Experimental cue to WLC principle

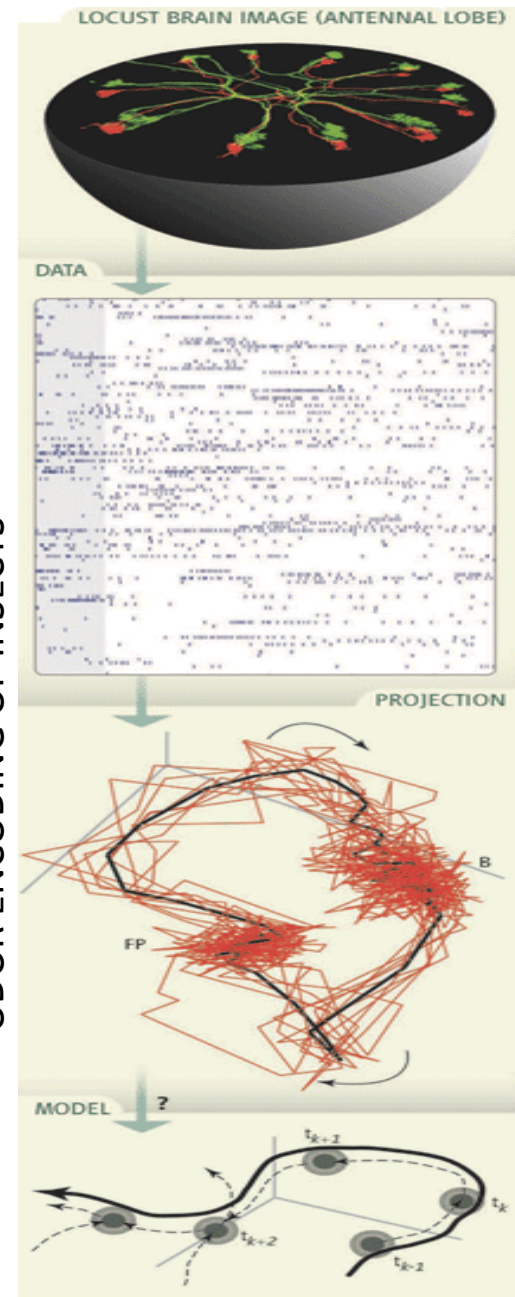
The temporal patterns produced by three simultaneously sampled PNs in the locust antennal lobe when two different odors are presented. The horizontal bar indicates the time interval when the stimulus was presented (see for details: M. Rabinovich et al., PRL , 2001



Winnerless Competition Principle



Rabinovich et al., PRL 2001; SCIENCE 2008

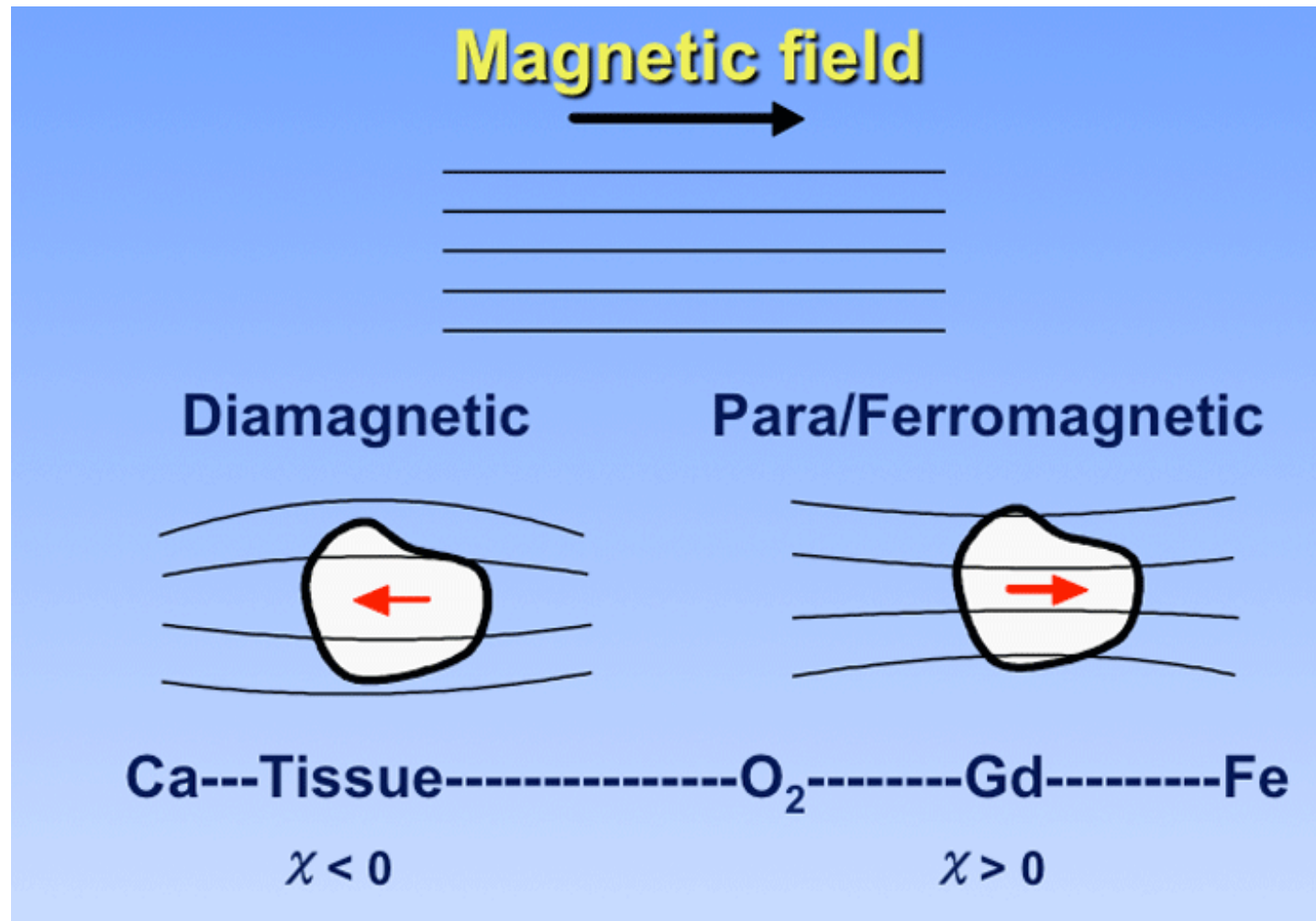


fMRI

Noninvasive studies of human brain function hold great potential to unlock mysteries of the human mind.

- Exploiting differences in magnetic susceptibility between *Oxygenated* and *Deoxygenated* blood (Blood Oxygenation Level–Dependent – *BOLD* –contrast), functional MRI (*fMRI*) detects metabolic activity, and by inference, neuronal activity, noninvasively throughout the brain. This technique generates complex data sets: ~100,000 locations, measured simultaneously hundreds of times, resulting in billions of pairwise relations, collected in multiple experimental conditions, and from dozens of participants per study.
- With this powerful technology in widespread use, data analysis has become the bottleneck for progress. What is the best way to find the mind in brain data?

During metabolic consumption of oxygen in the brain and weakly **diamagnetic oxyhemoglobin** releases O₂ and becomes strongly **paramagnetic deoxyhemoglobin**

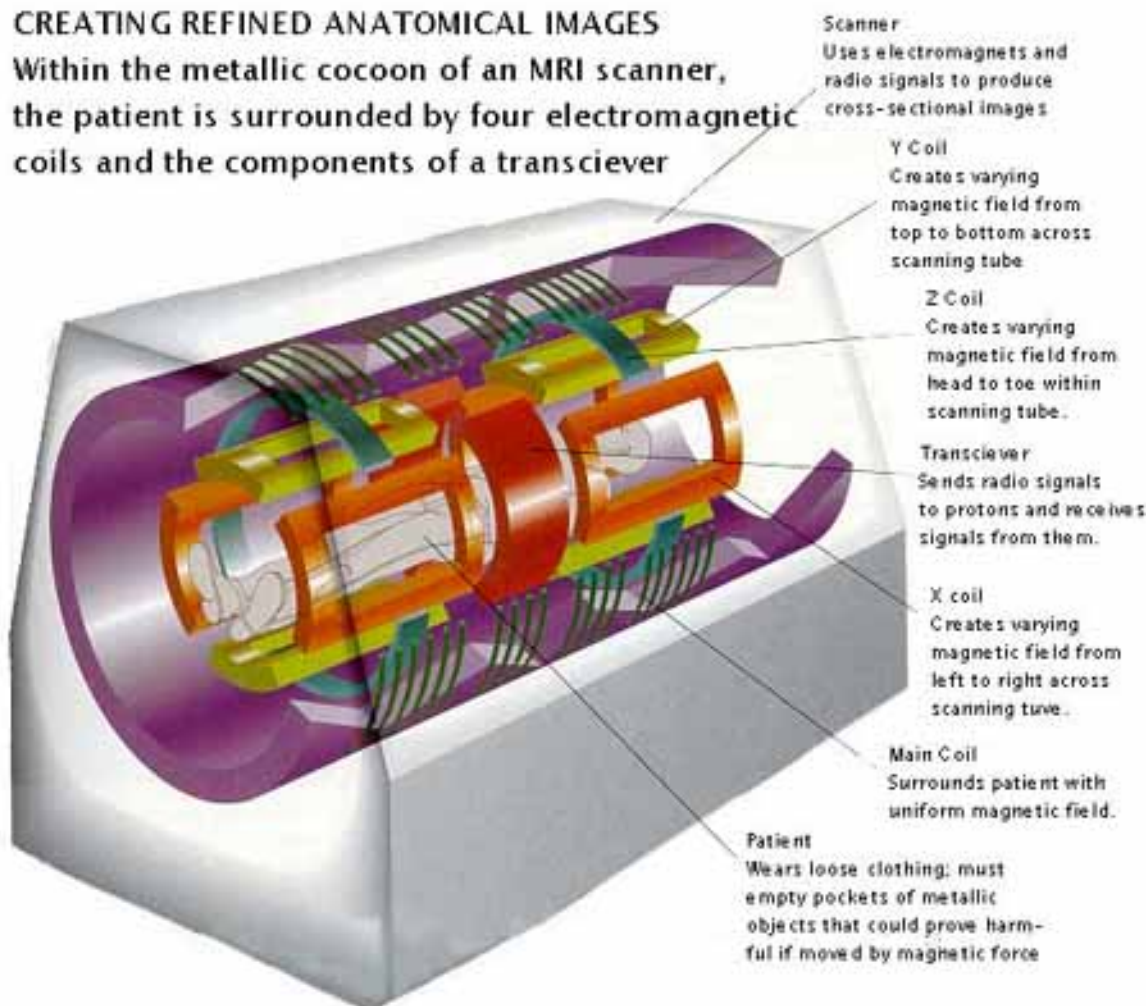


oxygenated and less oxygenated blood behave differently in the magnetic field of an MRI and this differential response is exploited to image relative arterial blood flow to different parts of the brain

Magnetic Property	Direction of Polarization (I) Relative to External Field	Relative Magnetic Susceptibility (χ) in ppm	Typical Materials
Diamagnetism	Opposite	-10	Water, fat, calcium, most biologic tissues
Paramagnetism	Same	+1	Molecular O ₂ , simple salts and chelates of metals (Gd, Fe, Mn, Cu), organic free radicals
Superparamagnetism	Same	+5000	Ferritin, hemosiderin, SPIO contrast agents
Ferromagnetism	Same	> 10,000	Iron, steel

CREATING REFINED ANATOMICAL IMAGES

Within the metallic cocoon of an MRI scanner,
the patient is surrounded by four electromagnetic
coils and the components of a transciever

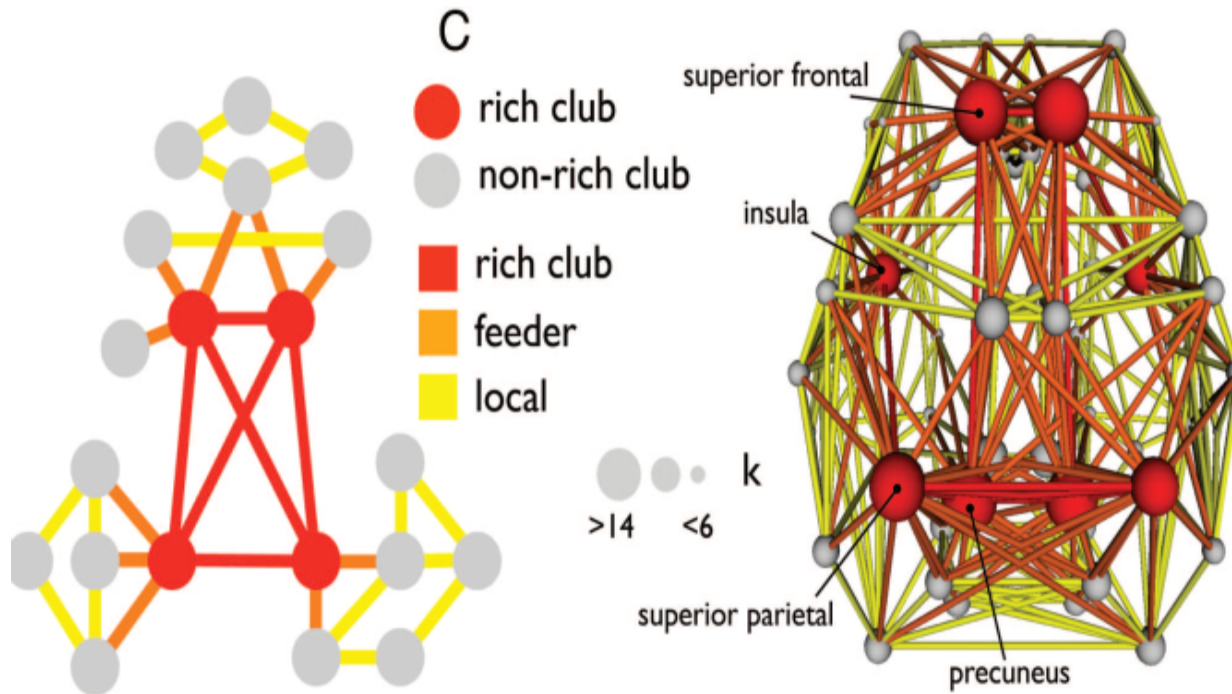


Jazz musician in an fMRI scanner

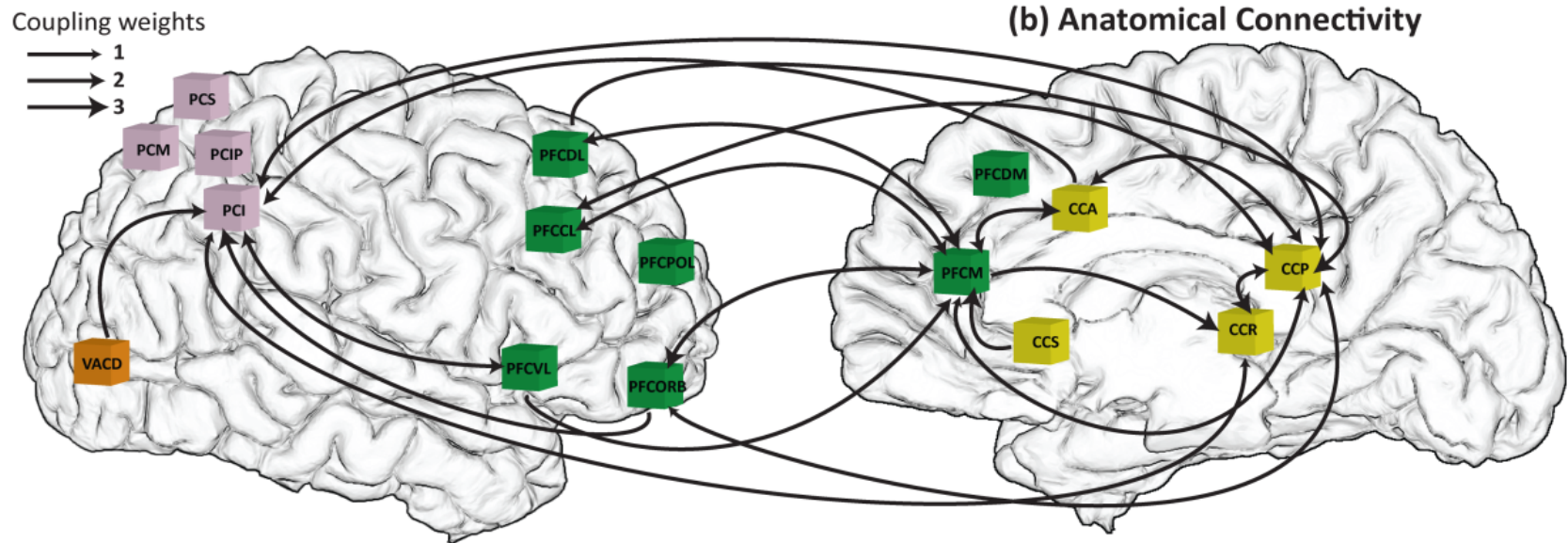
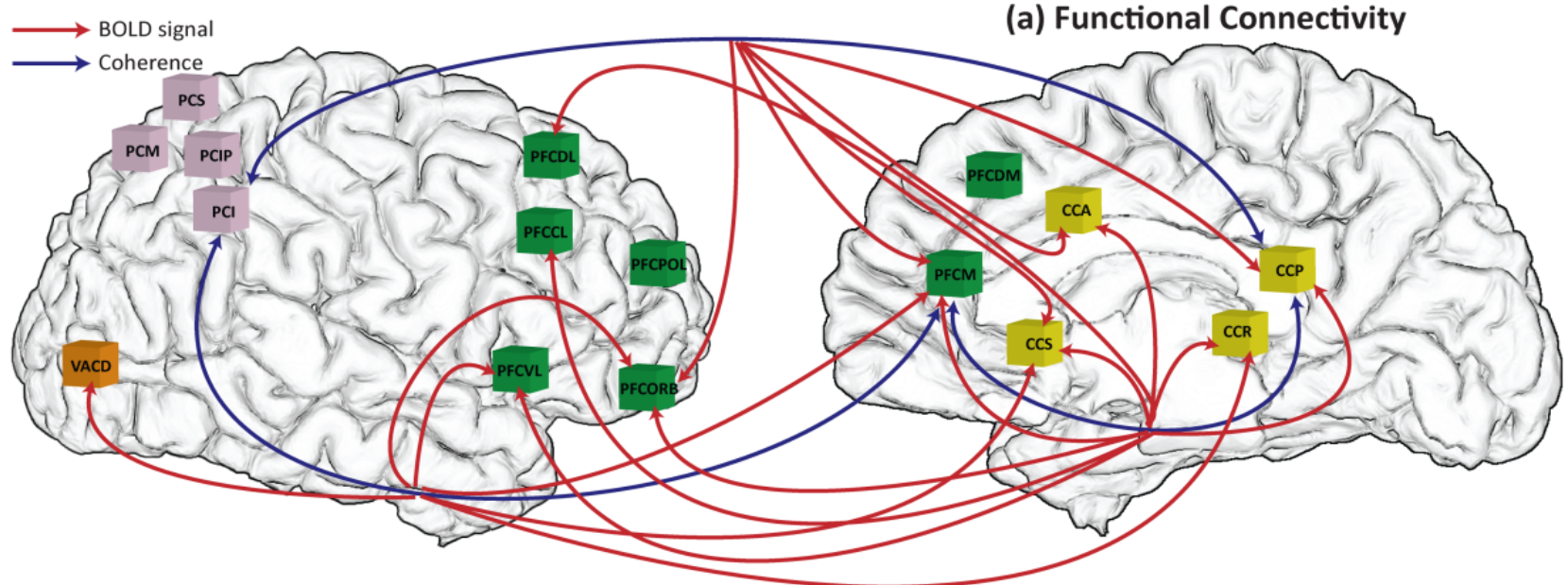


Limb CJ, Braun AR (2008) PLoS ONE 3:e1679

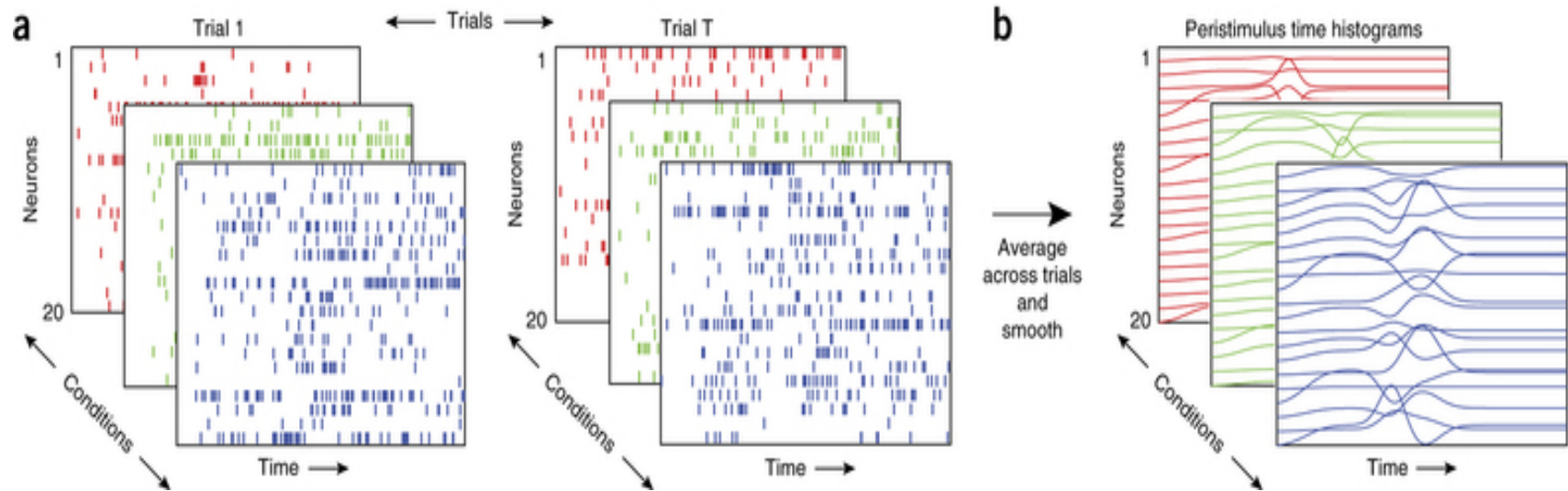
Inferring Brain Functional Networks from Neuroimaging Data



The selected rich club included bilateral precuneus, superior frontal cortex, insular cortex, and superior parietal cortex (*de Reus, van den Heuvel, Neuroimage, 2013*)



Population analyses and dimensionality reduction



Cunningham & Byron, Nature Neuroscience, 2014

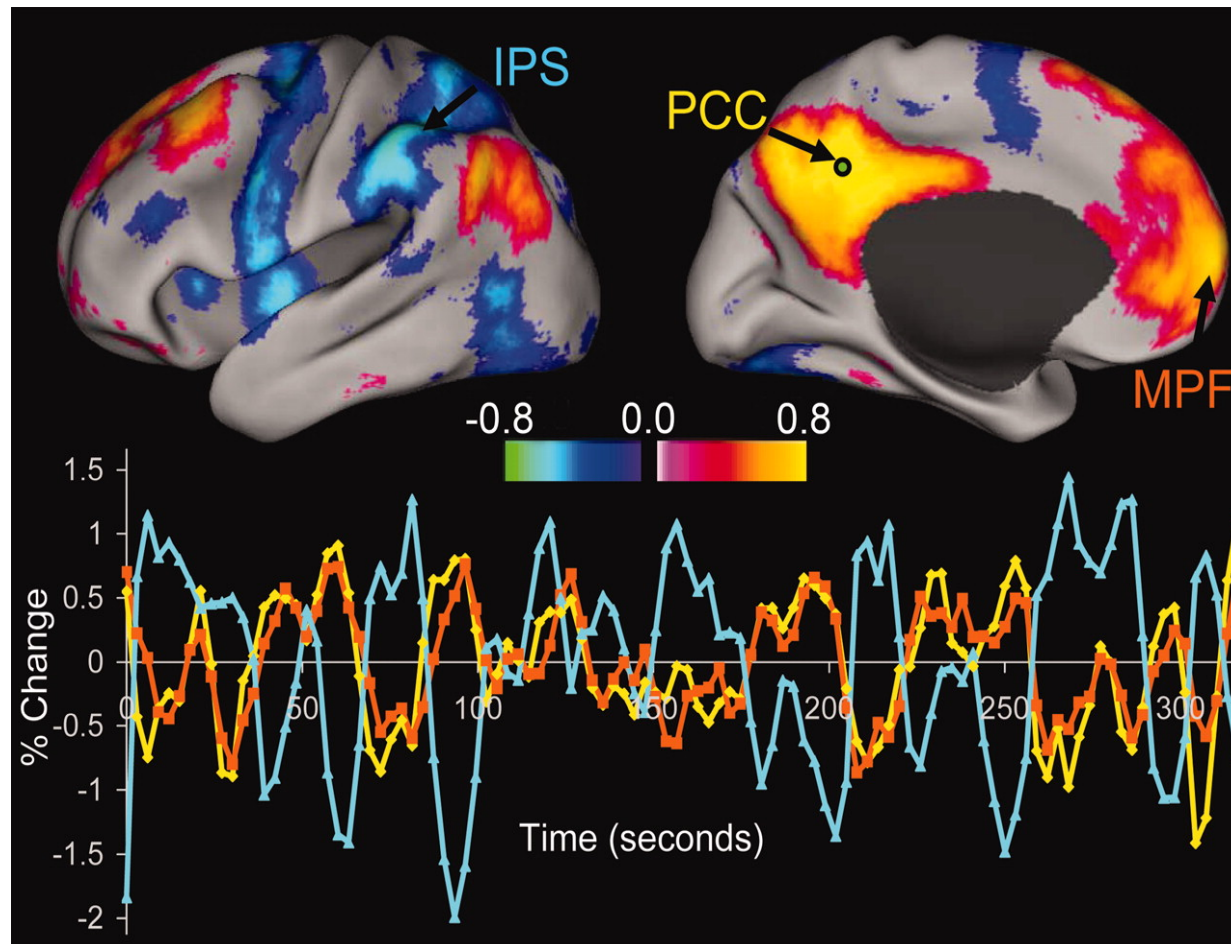
Neuronal activity clusterization – Principle components – modes dynamics

$$R(l,t) = \sum_{m=1}^M P^m(l,t) \quad (2.1)$$

$$\frac{dP^m}{dt} = P^m(l,t) \cdot \left[\tilde{\gamma}^m - \sum_{k=1}^M \tilde{\zeta}^{mk} P^k(l,t) \right], \quad (2.2)$$

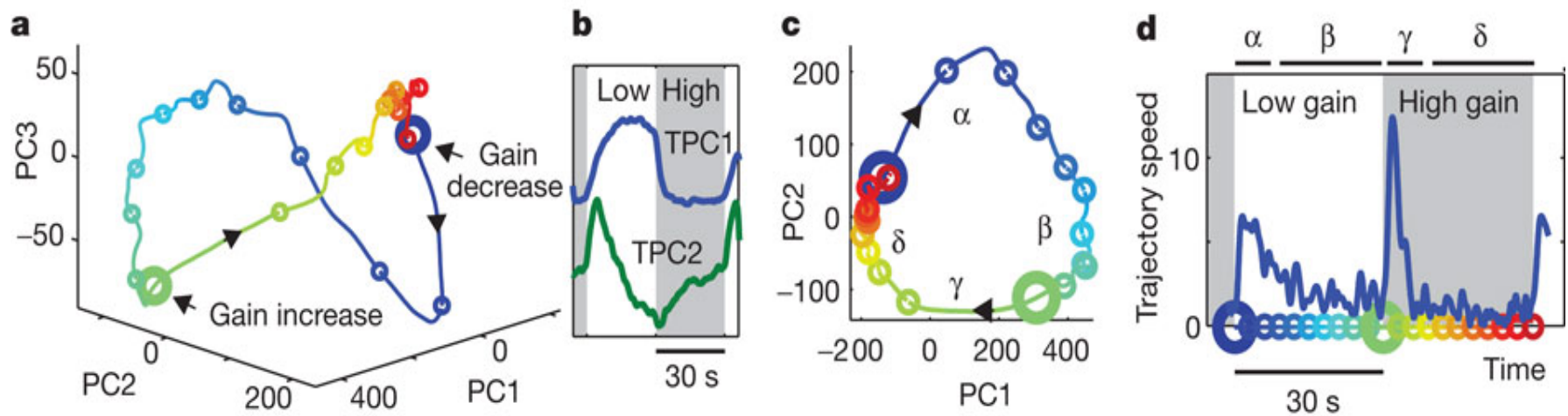
$P^m(l,t) = R^m(t)Q^m(l)$ is the m -th spatio-temporal mode that depends on time and is based on the set of discrete coordinates in the brain space (voxels coordinates), $R^m(t)$ represents the temporal evolution of the m -th mode whose temporal structure is represented by $Q^m(l)$, the projection function of the m -th mode, and M is the number of modes.

Spatio-temporal dynamics of resting modes



Fox et al, The human brain is intrinsically organized into dynamic, anticorrelated functional networks. PNAS, 102, 9673 (2005)

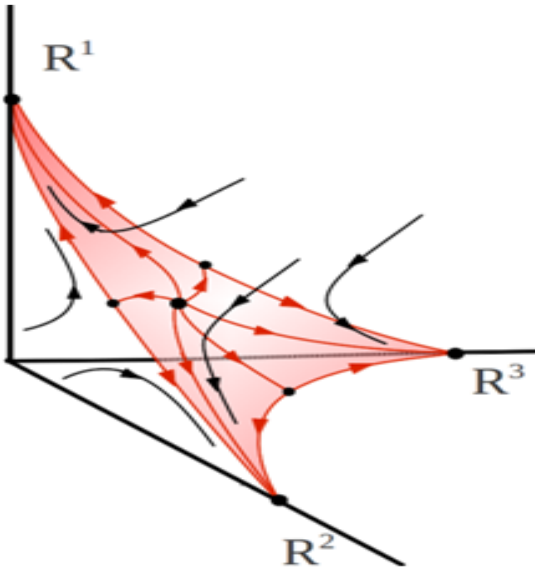
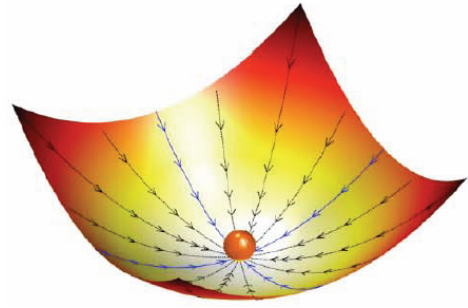
Low-dimensional representation of neural network dynamics during motor adaptation in zebrafish



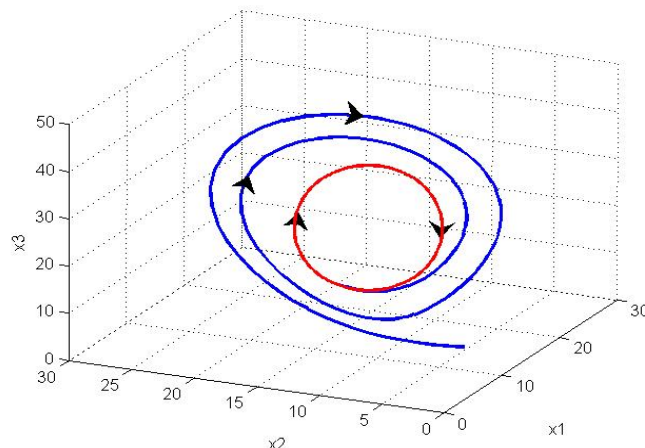
MB Ahrens et al. *Nature* **485**, 471-477, (2012) doi:10.1038/nature11057

Transient Nonlinear Dynamics versus Attractors

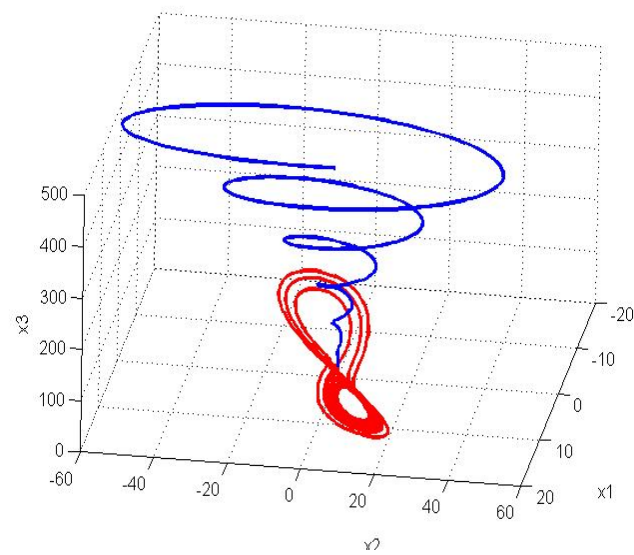
Historical remarks



Hopfield associative memory
– multistability (1982)

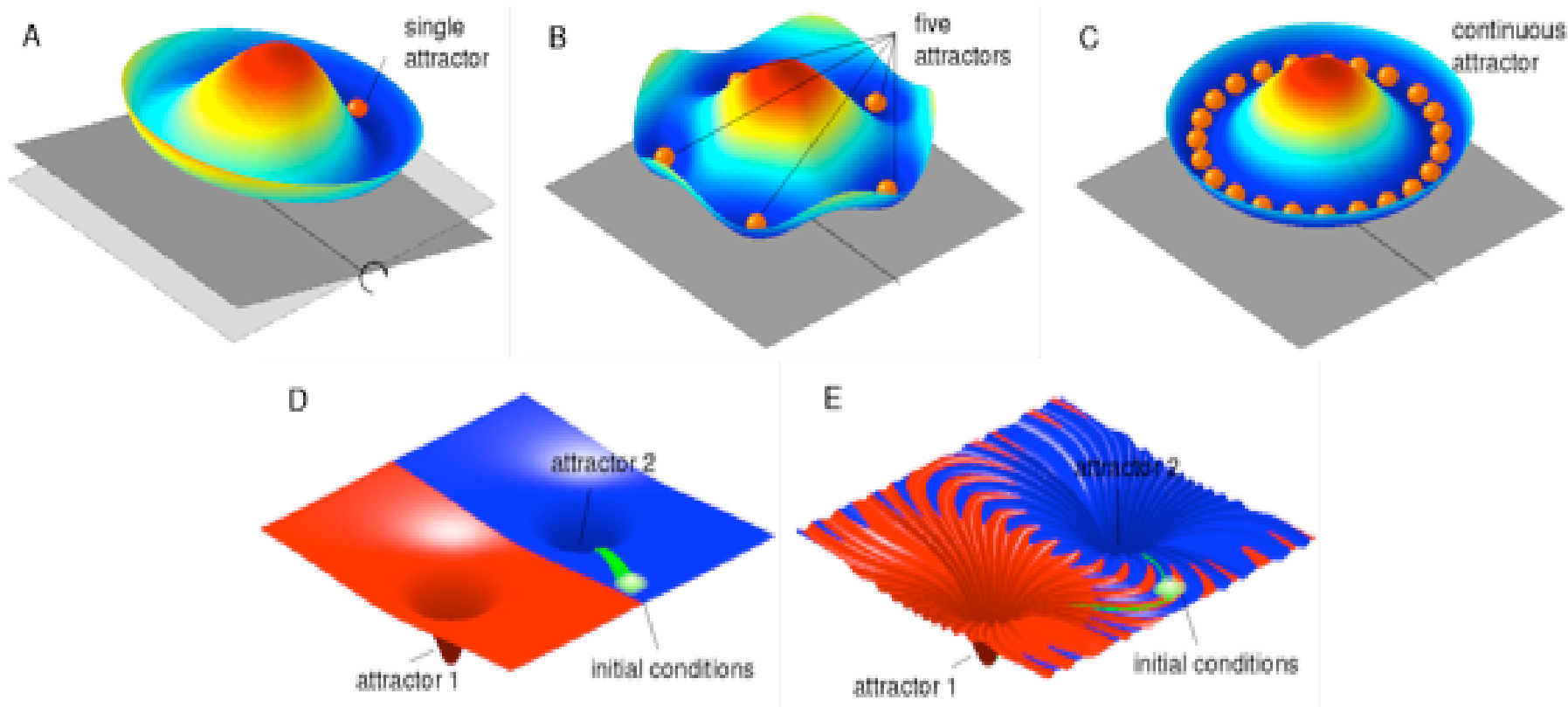


Some 3-body orbits
Poincare (1899)

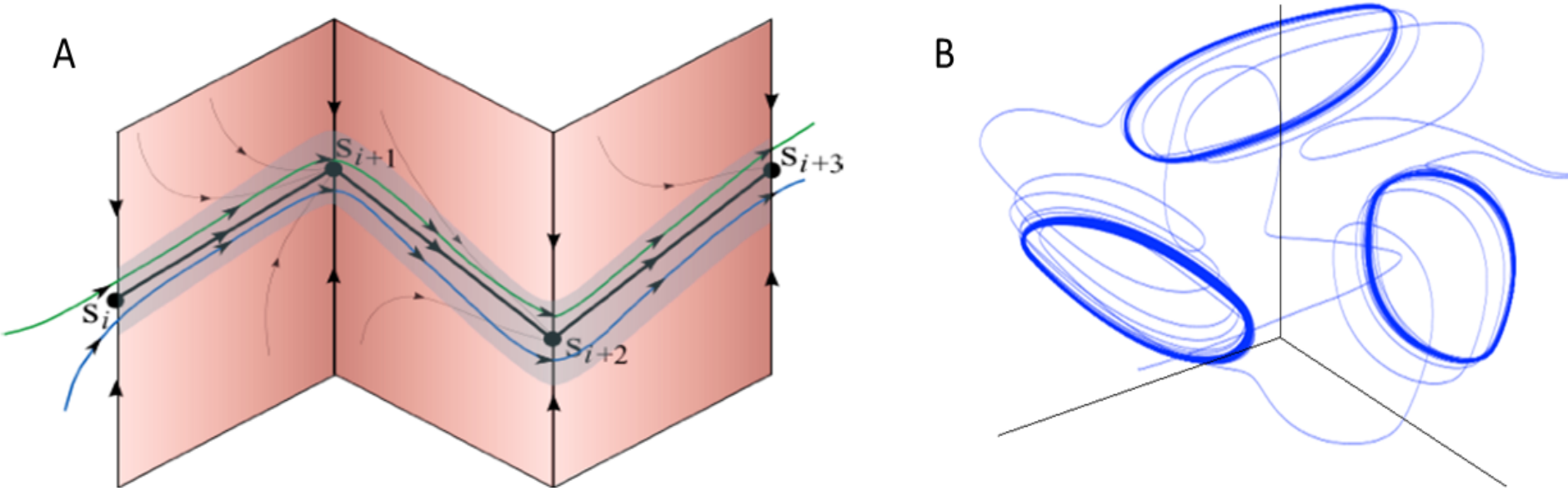


Strange attractor
Lorenz (1963)

Multistability



Stable Heteroclinic Channel

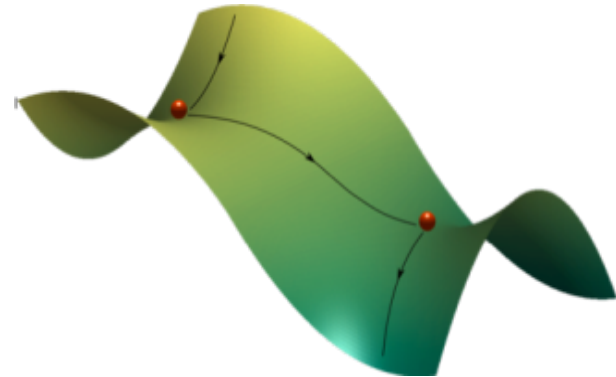
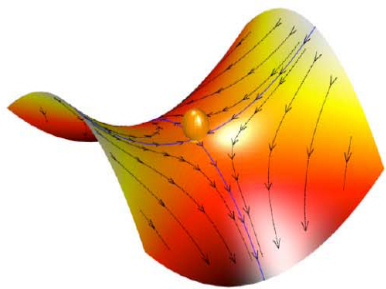


heteroclinic channel is an adequate mathematical object to represent robust transient dynamics, in the cognitive phase space.

A: sequence of metastable states representing the informational items, each metastable states is static – saddle fixed point. S_k is the number of the item.

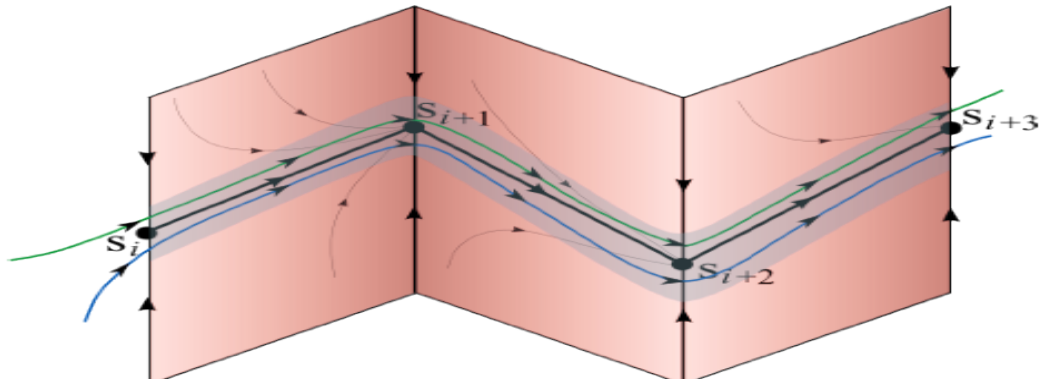
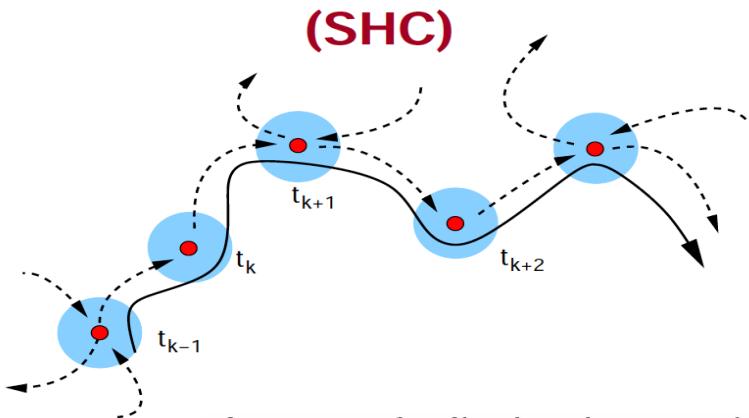
B: sequence of dynamical metastable states (the mathematical image of these informational items in this case is a saddle limit cycle)

COGNITIVE DYNAMICS ARE TRANSIENT – CHAIN OF METASTABLE STATES – *Robust Heteroclinic Channel*



A separatrix is a manifold (surface or curve) that refers to the boundary separating two modes of behavior in the phase space of a dynamical system.

Simple Heteroclinic Chain



A set of dissipative saddles that are sequentially connected by unstable separatrices. The stability of a channel means that trajectories in the channel do not leave it until the end of the channel is reached.

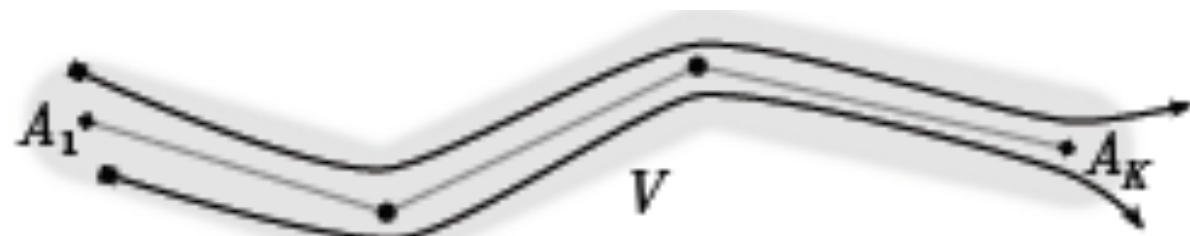
Afraimovich et al., Chaos, 2004; Rabinovich et al., SCIENCE 2008.

Working memory capacity

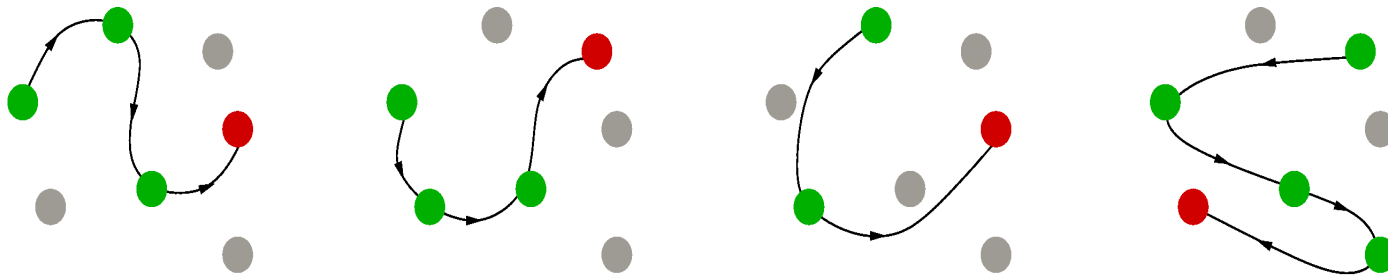
is the number of items in the chain that can be recalled without error – length of the information flow before it loses its stability

**Normal
form**

$$\dot{a}_i = a_i \left(\sigma_i(M, S) - \left(a_i + \sum_{j \neq i} \varrho_{ij}(M, S) a_j \right) \right)$$



Conditions for the Heteroclinic Channel Stability. Saddle value. Prediction



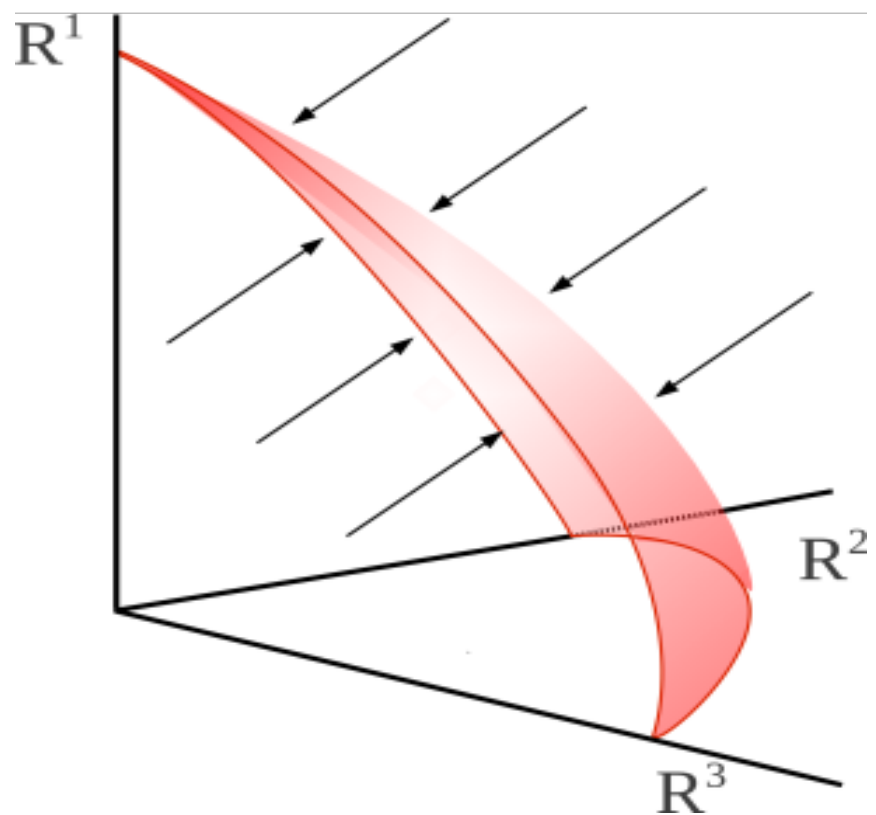
Different information inputs (external or internal stimuli) are represented in the phase space by different sequences of global modes activity – different chains of metastable states. The specific topology of the signal-dependent information flow is a key feature that helps to solve a problem of information flow stability against stationary noise.

Let the eigenvalues $\lambda_1^{(i)}, \dots, \lambda_n^{(i)}$ of the matrix of the system linearized at S_i be ordered in such a way that

$$\lambda_1^{(i)} > \dots \geq \operatorname{Re} \lambda_{m_i}^{(i)} > 0 > \operatorname{Re} \lambda_{m_i+1}^{(i)} \geq \dots \geq \operatorname{Re} \lambda_n^{(i)}$$

Saddle value: $-\frac{\operatorname{Re} \lambda_{m_i+1}^{(i)}}{\lambda_1^{(i)}} = \nu_i > 1$ compression stronger than stretching

Stable Simplex in the phase space LV model



Bifurcations in a simplex - 3D LV model

